



NOTE

Internal Medicine

Immunocytochemical evaluation of epithelial–mesenchymal transition in epithelial tumors of dogs and cats

Yu FURUSAWA¹⁾, Masashi TAKAHASHI¹⁾, Mariko SHIMA-SAWA²⁾, Hitoshi HATAI³⁾, Noriaki MIYOSHI³⁾, Osamu YAMATO²⁾ and Akira YABUKI^{1,2)*}

¹⁾Kagoshima University Veterinary Teaching Hospital, Joint Faculty of Veterinary Medicine, Kagoshima University, 1-21-24 Korimoto, Kagoshima 890-0065, Japan

²⁾Laboratory of Veterinary Clinical Pathology, Joint Faculty of Veterinary Medicine, Kagoshima University, 1-21-24 Korimoto, Kagoshima 890-0065, Japan

³⁾Laboratory of Veterinary Histopathology, Joint Faculty of Veterinary Medicine, Kagoshima University, 1-21-24 Korimoto, Kagoshima 890-0065, Japan

ABSTRACT. Epithelial–mesenchymal transition (EMT) plays a crucial role in metastasis of epithelial tumors; however, it is challenging to detect EMT by cytology. In the present study, EMT was visualized by fluorescence-immunocytochemistry (FICC). Air-dried smears from epithelial tumors of dogs (n=22) and cats (n=9) were stained using mouse monoclonal anti-E-cadherin and rabbit monoclonal anti-vimentin antibodies. Enzymatic immunohistochemistry (IHC) revealed that 51.6% (8/22 in dogs, 8/9 in cats) of the cases showed EMT. In dogs, FICC could detect EMT in 62.5% (5/8) of those cases. In cats, FICC could detect EMT in 100% (8/8) of the cases. In conclusion, the present FICC method could successfully detect EMT using conventional air-dried cytology smear slides.

KEY WORDS: cytology, E-cadherin, epithelial-mesenchymal transition, immunocytochemistry, vimentin

J. Vet. Med. Sci.

83(9): 1363–1368, 2021

doi: 10.1292/jvms.21-0021

Received: 11 January 2021

Accepted: 21 June 2021

Advanced Epub:

8 July 2021

Epithelial–mesenchymal transition (EMT) plays a crucial role in tumor metastasis and progression. It is a dynamic process that occurs during epithelial tumor development and invasion, which has been associated with the aggressive clinical behavior of tumors [6]. EMT is a phenomenon in which epithelial cells acquire mesenchymal traits, and loss of E-cadherin, which facilitates the mobility and invasion of epithelial tumor cells, is seen in the course of EMT during tumor progression [1, 4, 15, 16, 18]. In addition, vimentin, an intermediate filament in mesenchymal cells, is expressed as EMT progresses in epithelial malignant tumors [11, 18]. In human medicine, EMT has been associated with the metastatic process in many different types of epithelial malignant tumors, such as mammary carcinoma and squamous cell carcinoma (SCC) [2, 8]. In small animal medicine, histopathological studies have suggested that EMT occurs during the metastatic process of canine prostate carcinoma and canine mammary carcinoma [3, 9]. Other studies have reported that EMT contributes to aggressive canine and feline oral SCC [5, 7].

Aging in dogs and cats causes an upsurge in cancer onset. Because elderly small animals have higher risks involved in invasive examination procedures, such as anesthesia and exploratory surgery, better non-invasive examinations are required. Cytology is a non-invasive and cost-effective method for the diagnosis of neoplastic diseases and can presume a certain level of tumor malignancy. However, prediction of tumor prognosis in a conventional cytological manner is challenging. Immunocytochemistry (ICC) is a useful tool in advanced diagnostic cytology, and non-invasive prediction of tumor metastasis might be possible by utilizing this technique. The present study targeted E-cadherin and vimentin as markers for the evaluation of EMT using ICC, and the results were compared with those obtained by standard immunohistochemistry.

The present experiments were conducted with the approval of the committee of the Veterinary Clinical Research of Kagoshima University, Japan (Accession No. KVH190001). Cytologic smears were prepared from surgical biopsy specimens. These smears were thoroughly air-dried and stored at -30°C until use. The surgically removed biopsy specimens were fixed in formalin and submitted to a histopathology laboratory. All histopathological diagnoses were made by veterinary pathologists without prior knowledge of cytological findings. TNM staging was applied to all cases that were diagnosed as malignant tumors, and these cases were evaluated for metastasis to other organs containing regional lymph nodes. The stages were determined during the first examination of the cases.

*Correspondence to: Yabuki, A.: yabu@vet.kagoshima-u.ac.jp

©2021 The Japanese Society of Veterinary Science



This is an open-access article distributed under the terms of the Creative Commons Attribution Non-Commercial No Derivatives (by-nc-nd) License. (CC-BY-NC-ND 4.0: <https://creativecommons.org/licenses/by-nc-nd/4.0/>)

Samples were randomly collected from dogs and cats that were admitted to Kagoshima University Veterinary Teaching Hospital, Japan, and selected. The inclusion criteria were as follows: 1) epithelial tumors that were clearly diagnosed using histopathology, 2) tumor malignancy was clearly determined using histopathology, 3) cytological diagnosis was matched to the histopathological diagnosis, and 4) smear slides containing numerous epithelial tumor cells with good cytomorphological quality. The exclusion criteria were as follows: 1) non-epithelial tumors that were clearly diagnosed using histopathology, 2) malignancy of the tumors could not be clearly determined using histopathology, 3) cytological diagnosis did not match the histopathological diagnosis, 4) more than one population of neoplastic cells was detected histologically and cytologically; 5) apparent inflammation, necrosis, and fibrosis were detected histologically and cytologically; and 6) cytological samples with poor cytomorphological quality. Based on these criteria, samples from dogs (n=22) and cats (n=9) were selected and used for the following analysis. Complete blood count and blood chemical analyses, including C-reactive protein levels for dogs, were performed to evaluate the general conditions and concomitant diseases in all these cases.

ICC was performed in accordance with the recently published method of the multiple fluorescent ICC (FICC) method [14]. The mouse monoclonal anti-human E-cadherin (clone 36, 1:100; BD Biosciences, Franklin Lakes, NJ, USA) and rabbit monoclonal anti-human vimentin (clone SP20, 1:200 dilution; Spring Bioscience, Pleasanton, CA, USA) were used as primary antibodies and incubated for 15 min at 37°C. Alexa Fluor 488-conjugated goat anti-mouse IgG (1:500 dilution, Life Technologies, Paisley, UK) and Alexa Fluor 594-conjugated donkey anti-rabbit IgG (1:500 dilution, Life Technologies) were used as secondary antibodies and incubated for 15 min at 37°C. All antibodies were diluted in a blocking solution containing 0.25% casein in 10 mM phosphate-buffered saline (PBS). Nuclei were counterstained with 4,6-diamidino-2-phenylindole (DAPI; Dojinkagaku, Tokyo, Japan). For negative controls, normal mouse IgG (Dakocytomation, Glostrup, Denmark) and normal rabbit IgG (Dakocytomation) were used instead of the primary antibodies. Stained slides were examined under a fluorescence microscope (BX-53; Olympus, Tokyo, Japan) equipped with a cooled charge-coupled device camera (DP-73; Olympus). Images were captured and processed using imaging software (cellSens Standard; Olympus).

For standard IHC, the same primary antibodies as mentioned in ICC were used. Antibodies for E-cadherin and vimentin were diluted at 1:200 in a blocking solution of 0.25% casein/PBS and incubated overnight at 4°C. Peroxidase-polymer-conjugated universal antibody (anti-mouse IgG and anti-rabbit IgG, ready to use; Simple Stain MAX PO, Nichirei Biosciences, Tokyo, Japan) was used as a secondary antibody and incubated for 30 min at room temperature. Immunoreactivity was colorized using 3,3-diaminobenzidine (DAB) chromogen (DAB-buffer tablet; Merck, Darmstadt, Germany). For negative controls, normal mouse IgG (Dakocytomation) and rabbit IgG (Dakocytomation) were used instead of the primary antibodies.

In the present study, the attenuation of E-cadherin and the expression of vimentin in epithelial tumor cells were defined as EMT. The attenuation of E-cadherin could be evaluated by comparing the tumor cells on the same slide because clear positive signals were observed in tumor cells even though the tissues showed EMT. For the expression of vimentin, non-malignant mesenchymal cells in the same slide could be used as positive control cells. If non-malignant mesenchymal cells could not be observed, especially in the FICC slide, a few macrophages in the same slide could be used as positive control cells. In addition to these internal positive cells, positive signals were determined by comparison with the negative control slides prepared from the same tissue. The relationship between metastasis and EMT was statistically evaluated through conducting Fisher's exact test using the PASW software (IBM SPSS Statistics, Armonk, NY, USA).

In all 31 cases, immunosignals for E-cadherin and/or vimentin were clearly detected in both FICC and IHC, and these results are summarized in Table 1. In the IHC results, EMT could be observed in 16 out of 31 cases (51.6%), which is characterized by an attenuation of E-cadherin and expression of vimentin. Among the positive results, eight samples were from dogs, which means 36.4% (8/22) of the canine cases showed EMT. The remaining eight positive results were from cats, which means 88.9% (8/9) of the feline cases showed EMT. In these cases, the epithelial tumor cells in the IHC images showed low membranous immunoreactivity for E-cadherin and a clear positive signal for vimentin. The same staining pattern for E-cadherin and vimentin was also observed in images obtained by ICC (Figs. 1 and 2). In the non-EMT malignant cases, tumor cells showed a clear positive immunoreactivity for E-cadherin but were negative for vimentin in both IHC and ICC (Fig. 3). FICC results from three dogs (tubulopapillary carcinoma of the mammary gland, follicular adenoma of the thyroid gland, and adenosquamous carcinoma of the lung) were in disagreement with the IHC results (Fig. 4 and Table 1).

The sensitivity and specificity of FICC for detecting EMT were statistically calculated by comparing the FICC results with IHC results. Sensitivities for all cases, dogs, and cats were 81.2%, 62.5%, and 100%, respectively. The specificities were 100% for all cases, dogs, and cats. Upon statistically evaluating the relationship between metastasis and EMT, it was found that there were no significant relationships between these two properties in all three groups, i.e., all cases, dogs, and cats.

ICC can be visualized using enzymatic and fluorescent markers [12–14], and ICC in this study was visualized using fluorescent markers. Although enzymatic ICC can be performed without special equipment, it has some limitations in the evaluation of the EMT using cytology smear slides. The attenuation of E-cadherin and expression of vimentin in the tumor cells have been defined as a characteristic of EMT [10]; however, it is difficult to evaluate this phenomenon by enzymatic ICC, since enzymatic ICC usually detects only one antigen in one slide, and at least three slides are needed to visualize the staining of E-cadherin and vimentin, and the general findings in Giemsa stain. Additionally, the cytomorphology of the conventional enzymatic ICC is ambiguous because the immunosignals are usually colorized as dark brown spots by the reaction with diaminobenzidine. However, these limitations of enzymatic ICC could be overcome using fluorescence techniques. Simultaneous detection of two antigens in one cytology smear from dogs and cats has previously been tried for the dual detection of CD3 and CD79α [12], and that of cytokeratin and vimentin [14], and it was reported that the sensitivity and specificity of FICC was superior to that of enzymatic

Table 1. Findings of the all cases examined by immunohistochemistry (IHC) and fluorescence immunocytochemistry (FICC)

Sites/species	Histopathological diagnosis	IHC		FICC		Agreement	Metastasis
		E-cad	Vim	E-cad	Vim		
Mammary gland/dog	Tubulopapillary carcinoma	At	Posi	non-At	Nega	×	non-Me
Mammary gland/dog	Tubulopapillary carcinoma	non-At	Nega	non-At	Nega	○	non-Me
Mammary gland/dog	Benign mixed tumor	non-At	Nega	non-At	Nega	○	non-Me
Mammary gland/dog	Benign mixed tumor	non-At	Nega	non-At	Nega	○	non-Me
Mammary gland/dog	Complex adenoma	non-At	Nega	non-At	Nega	○	non-Me
Mammary gland/dog	Simple adenoma	At	Posi	At	Posi	○	non-Me
Mammary gland/dog	Lipid-rich carcinoma	non-At	Nega	non-At	Nega	○	non-Me
Gingiva/dog	Squamous cell carcinoma	At	Posi	At	Posi	○	non-Me
Gingiva/dog	Squamous cell carcinoma	At	Posi	At	Posi	○	Me
Tonsil/dog	Squamous cell carcinoma	At	Posi	At	Posi	○	Me
Rectum/dog	Adenocarcinoma	non-At	Nega	non-At	Nega	○	non-Me
Rectum/dog	Adenocarcinoma	non-At	Nega	non-At	Nega	○	non-Me
Rectum/dog	Adenocarcinoma	non-At	Nega	non-At	Nega	○	non-Me
Thyroid gland/dog	Follicular adenoma	At	Posi	non-At	Nega	×	non-Me
Thyroid gland/dog	Follicular carcinoma	non-At	Nega	non-At	Nega	○	non-Me
Perianal/dog	Perianal gland adenoma	non-At	Nega	non-At	Nega	○	non-Me
Perianal/dog	Perianal gland adenoma	non-At	Nega	non-At	Nega	○	non-Me
Perianal/dog	Anal sac adenocarcinoma	non-At	Nega	non-At	Nega	○	Me
Liver/dog	Hepatocellular carcinoma	non-At	Nega	non-At	Nega	○	non-Me
Trunk/dog	Trichoepithelioma	non-At	Nega	non-At	Nega	○	non-Me
Bladder/dog	Transitional cell carcinoma	At	Posi	At	Posi	○	non-Me
Lung/dog	Adenosquamous carcinoma	At	Posi	At	Nega	×	Me
Mammary gland/cat	Tubulopapillary carcinoma	At	Posi	At	Posi	○	Me
Mammary gland/cat	Tubulopapillary carcinoma	At	Posi	At	Posi	○	Me
Mammary gland/cat	Tubulopapillary carcinoma	At	Posi	At	Posi	○	Me
Mammary gland/cat	Tubulopapillary carcinoma	At	Posi	At	Posi	○	Me
Gingiva/cat	Squamous cell carcinoma	At	Posi	At	Posi	○	non-Me
Gingiva/cat	Squamous cell carcinoma	At	Posi	At	Posi	○	Me
Eyelid/cat	Squamous cell carcinoma	At	Posi	At	Posi	○	non-Me
Perineum/cat	Undifferentiated carcinoma	At	Posi	At	Posi	○	Me
Rectum/cat	Adenocarcinoma	non-At	Nega	non-At	Nega	○	Me

E-cad: E-cadherin, Vim: vimentin, At: attenuation of the E-cadherin, Posi: positive signals, Nega: negative signals, Ag: agreement, Me: metastasis.

ICC [14]. This method can also allow Giemsa staining after FICC, allowing the observer to recheck the morphology of the populations of interest after immunostaining [14].

FICC used in the present study demonstrated that this method could non-invasively evaluate EMT in epithelial tumor cells in dogs and cats. However, in dogs, FICC could not detect the EMT phenomenon in three cases (tubulopapillary carcinoma of the mammary gland, follicular adenoma of the thyroid gland, and adenosquamous carcinoma of the lung). In these cases, FICC could not detect the immunosignals of vimentin, although its expression was demonstrated by standard IHC. Since the degree of malignancy and metastasis did not seem to affect the difference between the findings of FICC and IHC, the amount of the cells that can be assessed might affect the detection of vimentin. The number of cells observed in cytology smears is usually quite small compared with that in the histopathological sections, and not all changes in the tumor tissues might be reflected in the cytology smears. Indeed, the three cases showed scattered vimentin-expression in the tumor cells. Two benign dogs showed EMT expression. Although EMT has also been demonstrated in non-malignant tissue lesions such as inflammation, fibrosis, and wound healing [17], samples with these lesions were excluded from the present analysis. No systemic inflammation was suspected in these two cases because the complete blood count and plasma concentration of C-reactive protein were normal. In addition, statistical analysis did not demonstrate a close relationship between EMT and metastasis in both dogs and cats. In the present study, although EMT was considered as a pathomolecular event in the neoplastic tissues, it was also suspected that EMT might be a molecular pathological event not only in invasion and metastasis but also other events such as the transition from benign tumors to malignant tumors. In cats, the EMT-phenomenon in all cases was successfully evaluated using FICC. Although EMT was frequently found in cats, this finding may be due to the small size of the samples and bias according to the type of tumors.

In conclusion, it was demonstrated that the present FICC method could successfully detect EMT using conventional air-dried cytology smear slides. Although a close relationship between EMT and malignancy could not be demonstrated because of the limited sample size, the significance of EMT as a metastatic or invasive marker might be different between the types of tumors or species. We believe that a non-invasive evaluation of the EMT using the FICC method would be useful in future prospective studies that investigate the clinical and diagnostic significance of EMT in neoplastic diseases in dogs and cats.

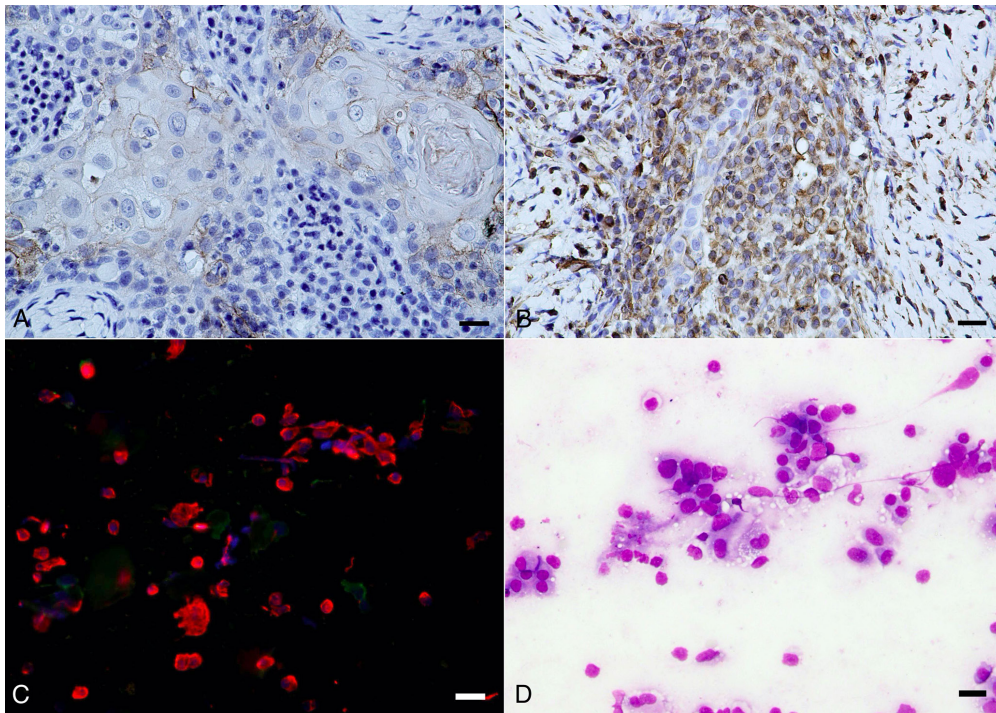


Fig. 1. Detection of the E-cadherin and vimentin in a squamous cell carcinoma of the tonsil from a dog. **(A)** Detection of E-cadherin by immunohistochemistry (IHC). **(B)** Detection of vimentin by IHC. **(C)** Simultaneous detection of E-cadherin (green signals) and vimentin (red signals) by fluorescence immunocytochemistry (FICC). **(D)** A standard Giemsa stain. Attenuation of the signals for E-cadherin and the distinct positive staining for vimentin in the tumor cells are observed in both IHC and FICC. In IHC panels: Diaminobenzidine chromogen, hematoxylin counterstain. In FICC panels: E-cadherin-Alexa 488, green; vimentin-Alexa 594, red; 4',6-diamidino-2-phenylindole (DAPI), blue. Bar=20 μ m.

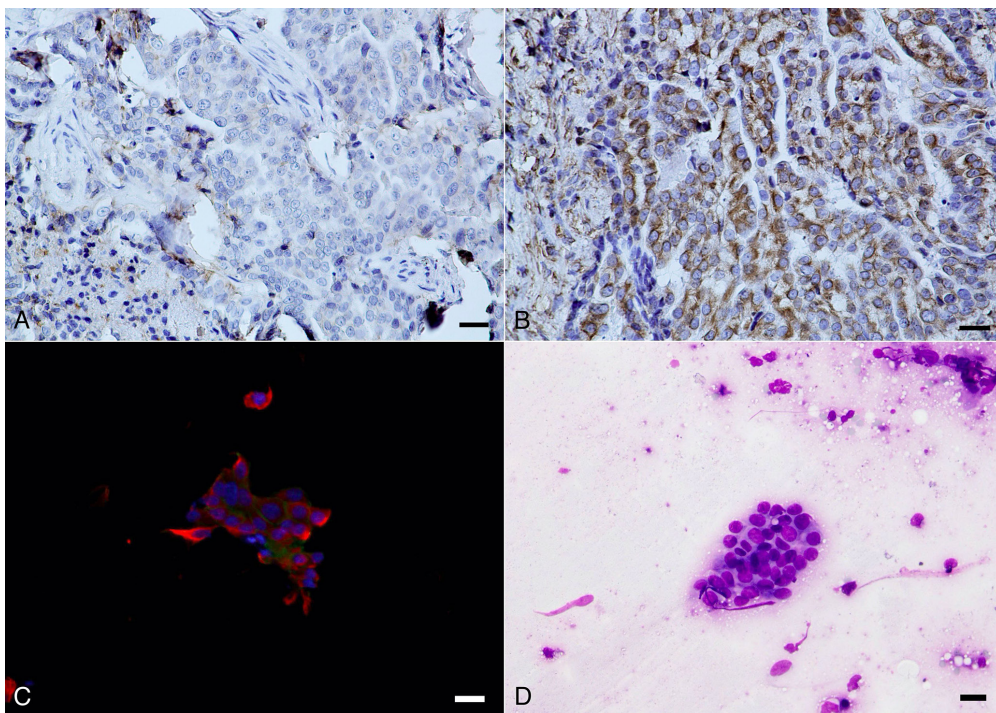


Fig. 2. Detection of E-cadherin and vimentin in tubulopapillary carcinoma of a mammary gland from a cat. **(A)** Detection of E-cadherin by immunohistochemistry (IHC). **(B)** Detection of vimentin by IHC. **(C)** Simultaneous detection of E-cadherin (green signals) and vimentin (red signals) by fluorescence immunocytochemistry (FICC). **(D)** A standard Giemsa stain. Attenuation of the signals for E-cadherin and the positive signals for vimentin in the tumor cells are observed in both IHC and FICC. In IHC panels: Diaminobenzidine chromogen, hematoxylin counterstain. In FICC panels: E-cadherin-Alexa 488, green; vimentin-Alexa 594, red; 4',6-diamidino-2-phenylindole (DAPI), blue. Bar=20 μ m.

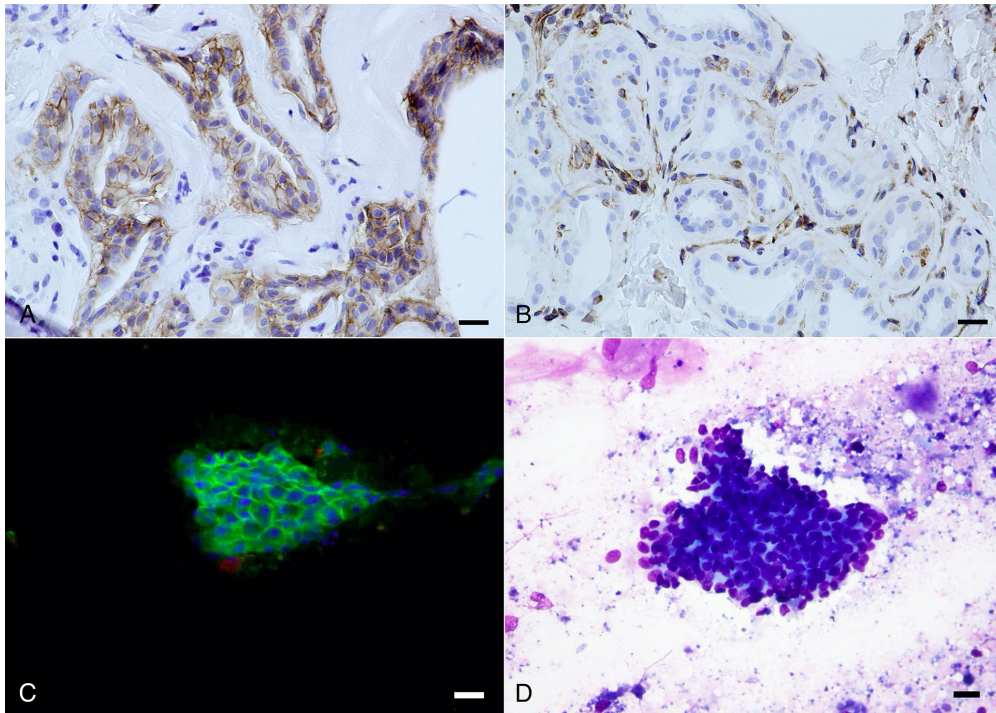


Fig. 3. Detection of E-cadherin and vimentin in benign mixed tumor of a mammary gland from a dog. **(A)** Detection of E-cadherin by immunohistochemistry (IHC). **(B)** Detection of vimentin by IHC. **(C)** Simultaneous detection of E-cadherin (green signals) and vimentin (red signals) by fluorescence immunocytochemistry (FICC). **(D)** A standard Giemsa stain. Epithelial tumor cells show positive signals for E-cadherin and negative signals for vimentin, and mesenchymal cells show positive signals for E-cadherin and negative signals for vimentin. These findings are similar in both IHC and FICC. In IHC panels: Diaminobenzidine chromogen, hematoxylin counterstain. In FICC panels: E-cadherin-Alexa 488, green; vimentin-Alexa 594, red; 4',6-diamidino-2-phenylindole (DAPI), blue. Bar=20 μ m.

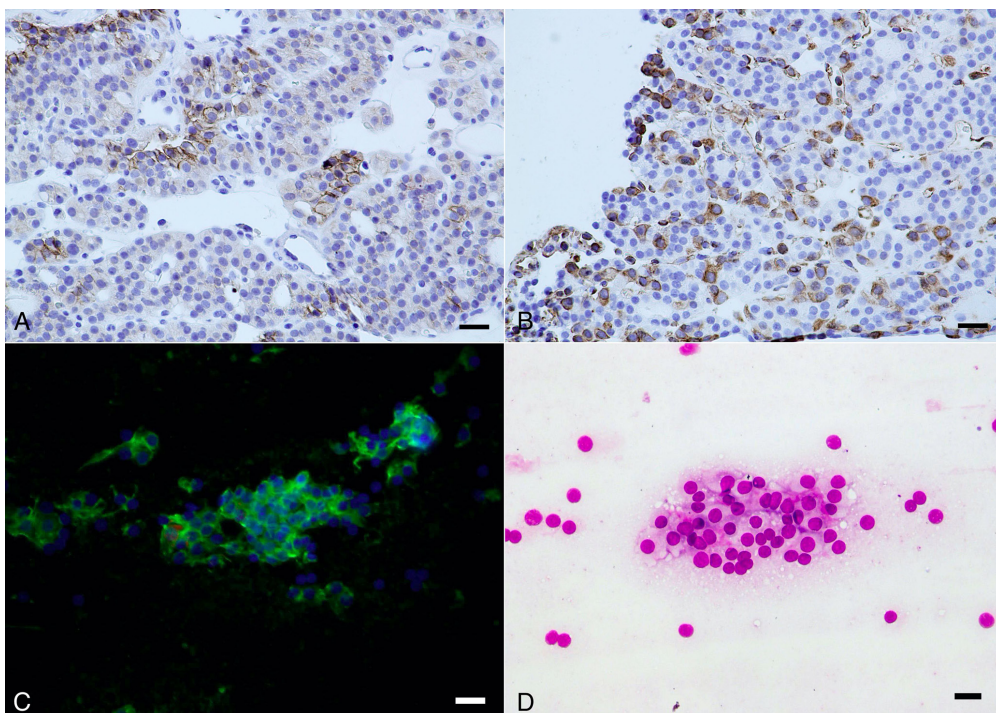


Fig. 4. Detection of E-cadherin and vimentin in follicular adenoma of the thyroid gland from a dog. **(A)** Detection of E-cadherin by immunohistochemistry (IHC). **(B)** Detection of vimentin by IHC. **(C)** Simultaneous detection of E-cadherin (green signals) and vimentin (red signals) by fluorescence immunocytochemistry (FICC). **(D)** A standard Giemsa stain. Attenuation of the signals for E-cadherin in the tumor cells are observed in both immunohistochemistry (IHC) and FICC. In the detection of the vimentin, positive signals are sporadically observed in the tumor cells in IHC, but no signals are observed in FICC. In IHC panels: Diaminobenzidine chromogen, hematoxylin counterstain. In FICC panels: E-cadherin-Alexa 488, green; vimentin-Alexa 594, red; 4',6-diamidino-2-phenylindole (DAPI), blue. Bar=20 μ m.

DECLARATIONS OF CONFLICTING INTERESTS. The authors declared no potential conflicts of interest with respect to the research, authorship, and/or publication of this article.

REFERENCES

1. Berx, G. and van Roy, F. 2009. Involvement of members of the cadherin superfamily in cancer. *Cold Spring Harb. Perspect. Biol.* **1**: a003129. [[Medline](#)] [[CrossRef](#)]
2. Brilliant, Y. M., Brilliant, A. A. and Sazonov, S. V. 2017. [Epithelial cadherins and associated molecules in invasive lobular breast cancer]. *Arkh. Patol.* **79**: 12–18. [[Medline](#)] [[CrossRef](#)]
3. Fonseca-Alves, C. E., Kobayashi, P. E., Rivera-Calderón, L. G. and Laufer-Amorim, R. 2015. Evidence of epithelial-mesenchymal transition in canine prostate cancer metastasis. *Res. Vet. Sci.* **100**: 176–181. [[Medline](#)] [[CrossRef](#)]
4. Guarino, M., Rubino, B. and Ballabio, G. 2007. The role of epithelial-mesenchymal transition in cancer pathology. *Pathology* **39**: 305–318. [[Medline](#)] [[CrossRef](#)]
5. Harris, K., Gelberg, H. B., Kiupel, M. and Helfand, S. C. 2019. Immunohistochemical features of epithelial-mesenchymal transition in feline oral squamous cell carcinoma. *Vet. Pathol.* **56**: 826–839. [[Medline](#)] [[CrossRef](#)]
6. Larue, L. and Bellacosa, A. 2005. Epithelial-mesenchymal transition in development and cancer: role of phosphatidylinositol 3' kinase/AKT pathways. *Oncogene* **24**: 7443–7454. [[Medline](#)] [[CrossRef](#)]
7. Nagamine, E., Hirayama, K., Matsuda, K., Okamoto, M., Ohmachi, T., Uchida, K., Kadosawa, T. and Taniyama, H. 2017. Invasive front grading and epithelial-mesenchymal transition in canine oral and cutaneous squamous cell carcinomas. *Vet. Pathol.* **54**: 783–791. [[Medline](#)] [[CrossRef](#)]
8. Pyo, S. W., Hashimoto, M., Kim, Y. S., Kim, C. H., Lee, S. H., Johnson, K. R., Wheelock, M. J. and Park, J. U. 2007. Expression of E-cadherin, P-cadherin and N-cadherin in oral squamous cell carcinoma: correlation with the clinicopathologic features and patient outcome. *J. Craniomaxillofac. Surg.* **35**: 1–9. [[Medline](#)] [[CrossRef](#)]
9. Raposo-Ferreira, T. M. M., Brisson, B. K., Durham, A. C., Laufer-Amorim, R., Kristiansen, V., Puré, E., Volk, S. W. and Sorenmo, K. 2018. Characteristics of the epithelial-mesenchymal transition in primary and paired metastatic canine mammary carcinomas. *Vet. Pathol.* **55**: 622–633. [[Medline](#)] [[CrossRef](#)]
10. Ribatti, D., Tamma, R. and Annese, T. 2020. Epithelial-mesenchymal transition in cancer: A historical overview. *Transl. Oncol.* **13**: 100773. [[Medline](#)] [[CrossRef](#)]
11. Satelli, A. and Li, S. 2011. Vimentin as a potential molecular target in cancer therapy Or Vimentin, an overview and its potential as a molecular target for cancer therapy. *Cell. Mol. Life Sci. CMLS* **68**: 3033–3046. [[Medline](#)] [[CrossRef](#)]
12. Sawa, M., Yabuki, A., Setoguchi, A. and Yamato, O. 2015. Development and application of multiple immunofluorescence staining for diagnostic cytology of canine and feline lymphoma. *Vet. Clin. Pathol.* **44**: 580–585. [[Medline](#)] [[CrossRef](#)]
13. Sawa, M., Inoue, M., Yabuki, A., Kohyama, M., Miyoshi, N., Setoguchi, A. and Yamato, O. 2017. Rapid immunocytochemistry for the detection of cytokeratin and vimentin: assessment of its diagnostic value in neoplastic diseases of dogs. *Vet. Clin. Pathol.* **46**: 172–178. [[Medline](#)] [[CrossRef](#)]
14. Sawa, M., Yabuki, A., Kohyama, M., Miyoshi, N. and Yamato, O. 2018. Rapid multiple immunofluorescent staining for the simultaneous detection of cytokeratin and vimentin in the cytology of canine tumors. *Vet. Clin. Pathol.* **47**: 326–332. [[Medline](#)] [[CrossRef](#)]
15. Scanlon, C. S., Van Tubergen, E. A., Inglehart, R. C. and D'Silva, N. J. 2013. Biomarkers of epithelial-mesenchymal transition in squamous cell carcinoma. *J. Dent. Res.* **92**: 114–121. [[Medline](#)] [[CrossRef](#)]
16. Stemmler, M. P. 2008. Cadherins in development and cancer. *Mol. Biosyst.* **4**: 835–850. [[Medline](#)] [[CrossRef](#)]
17. Stone, R. C., Pastar, I., Ojeh, N., Chen, V., Liu, S., Garzon, K. I. and Tomic-Canic, M. 2016. Epithelial-mesenchymal transition in tissue repair and fibrosis. *Cell Tissue Res.* **365**: 495–506. [[Medline](#)] [[CrossRef](#)]
18. Zeisberg, M. and Neilson, E. G. 2009. Biomarkers for epithelial-mesenchymal transitions. *J. Clin. Invest.* **119**: 1429–1437. [[Medline](#)] [[CrossRef](#)]